

Proceedings

Development and Characterization of Polyaniline/Hexamethylene Diisocyanate-Modified Graphene Oxide Nanocomposites [†]

Ana Maria Diez Pascual * and José Antonio Luceño-Sánchez

Departamento de Química Analítica, Química Física e Ingeniería Química, Facultad de Ciencias, Universidad de Alcalá, E-28871 Madrid, Spain; jose.luceno@uah.es

* Correspondence: am.diez@uah.es; Tel.: +34-918-856-430

[†] Presented at the 2nd International Online-Conference on Nanomaterials, 15–30 November 2020; Available online: <https://iocn2020.sciforum.net/>.

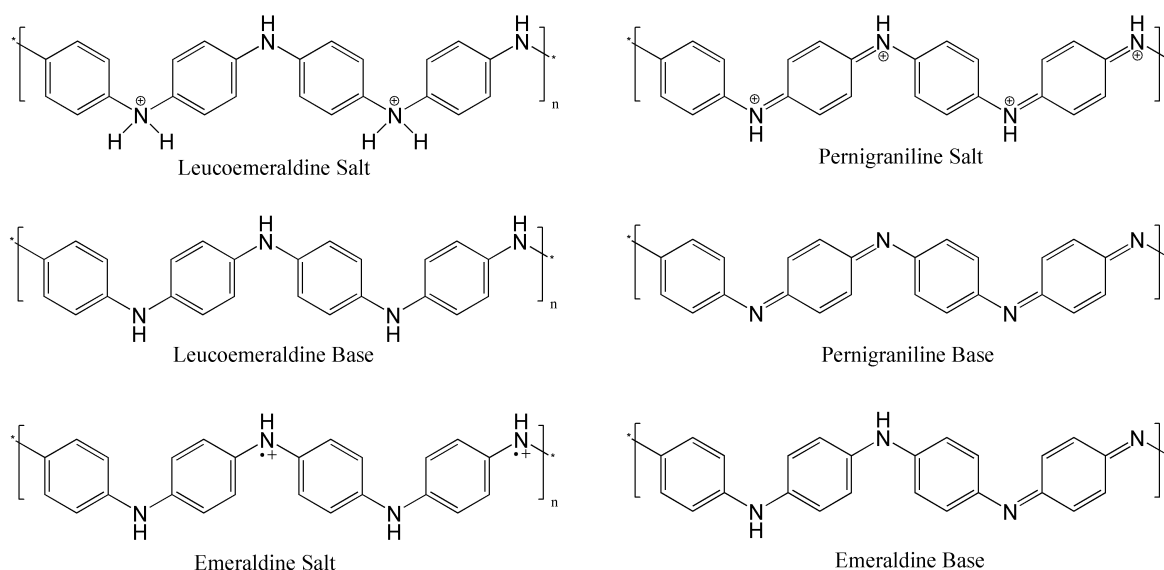
Published: 15 November 2020

Abstract: Polyaniline (PANI) is a cheap and widely used conducting polymer due to its exceptional electrical and optoelectronic properties. However, it is insoluble in conventional organic solvents and degrades at high temperature. To improve the performance of PANI, carbon-based nanomaterials such as graphene, graphene oxide (GO) and their derivatives can be incorporated in a PANI matrix. In this work, hexamethylene diisocyanate-modified GO has been used as reinforcement to prepare PANI/HDI-GO nanocomposites by means of in situ polymerization of aniline in the presence of HDI-GO followed by ultrasonication and solution casting. The effect of the HDI-GO functionalization degree and concentration on the final properties of the nanocomposites has been explored by scanning electron microscopy (SEM), Raman spectroscopy, X-ray diffraction (XRD), thermogravimetric analysis (TGA), tensile tests, and four-point probe measurements. An homogenous dispersion of the HDI-GO nanosheets has been found as well as very strong PANI-HDI-GO interactions via pi-pi stacking, H-bonding, and hydrophobic and electrostatic charge-transfer complexes. A continuous improvement in thermal stability and electrical conductivity was found with increasing nanomaterial concentration, the increments being larger with increasing HDI-GO degree of functionalization. The nanocomposites showed a very good combination of rigidity, strength, ductility and toughness. The approach developed herein opens up a versatile route to prepare multifunctional graphene-based nanocomposites with conductive polymers for a broad range of applications including photovoltaic organic solar cells.

Keywords: PANI; graphene oxide; nanocomposites; hexamethylene diisocyanate; characterization

1. Introduction

The properties and applicability of conducting polymers, such as polyaniline (PANI), are interesting facts that enables them to be employed as solar cells materials [1–3]. PANI represents one of the most studied polymers in the last decades, mostly due to its exceptional properties and its wide range of uses [1,4]. The synthesis of PANI can be accomplished by electrochemical or conventional approaches, and also the oxidation state of PANI can differ depending on the approach [5]. The possible oxidation states of PANI are depicted in Scheme 1: Leucoemeraldine Salt and Base, Pernigraniline Salt and Base, and Emeraldine Salt and Base.



Scheme 1. Structure of the different forms of PANI: the completely reduced leucoemeraldine, the completely oxidized pernigraniline and the emeraldine, in the base and salt forms. Taken from [6].

PANI presents good electrical properties, although it has low mechanical performance and undesirable bad solubility [7]. The addition of nanomaterials to PANI can improve its properties [8]; there are already studies adding graphene-based materials (graphene (G), graphene oxide (GO), and reduced graphene oxide (rGO)) to PANI via in situ polymerization or functionalization procedures [8–12], achieving an improvement of charge carriers transference and strong interfacial adhesion [13]. However, the the presence of graphene aggregates can reduce the material properties, so it is critical to enhance the dispersion of the nanomaterial. Previous works have focused on the development of functionalized graphene samples and preparation methods, looking for optimize the nanomaterials behavior [14–17].

In this work, a procedure to obtain PANI/GO nanocomposites, with a GO homogeneous dispersion, using in situ polymerization techniques is presented. The synthesis involves the use of ammonium peroxydisulfate as oxidizing agent, GO and hexamethylene diisocyanate-modified graphene oxide (HDI-GO) as the nanomaterials added to PANI, and acid medium. The interaction between PANI and HDI-GO or GO takes place via different options (π - π stacking, hydrogen bonding, and electrostatic and hydrophobic interactions). The nanomaterial synthesized were characterized to study the effect of graphene-based materials on the final properties.

2. Materials and Methods

2.1. Reagents

Aniline monomer ($C_6H_5NH_2$, >99%, $M_w = 93.13$ g/mol, $d_{25^\circ C} = 1.02$ g/cm³), ammonium persulfate ($(NH_4)_2S_2O_8$, 98%, $M_w = 228.20$ g/mol, $d_{25^\circ C} = 1.98$ g/cm³), triethylamine (TEA, >98%, $M_w = 101.193$ g/mol), H_2SO_4 , $KMnO_4$, P_2O_5 , $K_2S_2O_8$, and H_2O_2 were acquired from Sigma-Aldrich. Graphite powder was obtained from Bay Carbon, Inc. Hexamethylene diisocyanate (HDI, >99%, $M_w = 168.196$ g/mol) was purchased from Acros Organics. There were employed HPLC grade organic solvents, bought from Scharlau S.L. The deionized water was produced with a Milli-Q-Water-Purification-System. The chemicals were employed as received.

2.2. Synthesis of HDI-GO

The preparation of HDI-GO was carried out following the method showed in previous works [18,19], which is described briefly as: (1) synthesis of GO applying Hummers' method from graphite powder using H_2SO_4 , $K_2S_2O_8$, P_2O_5 and $KMnO_4$; (2) functionalization of GO with TEA as catalyst and HDI as reagent, added dropwise under 60 °C, inert atmosphere, and stirring during 12 h. The step 2

had two different ratios (GO:TEA:HDI) options, in order to study the functionalization degree (FD) effect in nanocomposite properties: (a) 1:1:1 (FD of 12.3%), and (b) 1:1:1 with a previous ultrasonic tip treatment (FD of 18.1%).

2.3. Synthesis of PANI/HDI-GO Nanocomposites

The synthesis procedure of the PANI/HDI-modified GO nanocomposites was an in situ polymerization of aniline monomers in acid medium in the presence of $(\text{NH}_4)_2\text{S}_2\text{O}_8$.

The first step involves the solution of 0.1 mL of aniline monomer with 25 mL of 1M HCl, and later the desired mass of HDI-GO (0.25, 0.50, 1.00, 2.50 or 5.00 mg). This mixture was ultrasonicated with a tip for 5 min and later an ultrasonic bath during 30 min. Parallely, 0.60 g of $(\text{NH}_4)_2\text{S}_2\text{O}_8$ were dispersed in 25 mL of 1M HCl, and later mixed dropwise to PANI-HDI-GO solution. The polymerization reaction, that starts when the solution takes green color, was carried out under stirring and in an ice bath during 12 h. In order to removal the residual polymers and oligomers, the reaction's products were filtrated and washed with deionized H_2O , ethanol, and hexane until colorless aspect, and later an oven was used to dry the products at 80 °C during 48 h.

In order to study the effect of HDI, and its FD, in the adding of GO, a sample of 5.00 mg pristine GO (10 wt%) and a PANI single samples were prepared, and also two different HDI-GO sets (called HDI-GO1 and HDI-GO6). Films based on the nanocomposite mixtures were obtained by dropping 5 mL of the sample in a glass and dried in the oven in the same conditions than the composites.

2.4. Instrumentation

The ultrasonication treatments were applied using a Selecta 3001208 ultrasonic bath and a 24 kHz Hielscher UP400S ultrasonic tip. A SU8000 Hitachi microscope was used for scanning electron microscopy (SEM) analysis. Raman spectra were obtained employed a Renishaw Raman microscope. The thermal stability was studied using a TA Instruments Q50s thermobalance.

3. Results

3.1. Morphology of Nanocomposites

The structures and morphology of the different samples (PANI, GO, HDI-GO and the nanocomposites obtained) were analyzed by SEM. The SEM micrographs are presented in Figure 1.

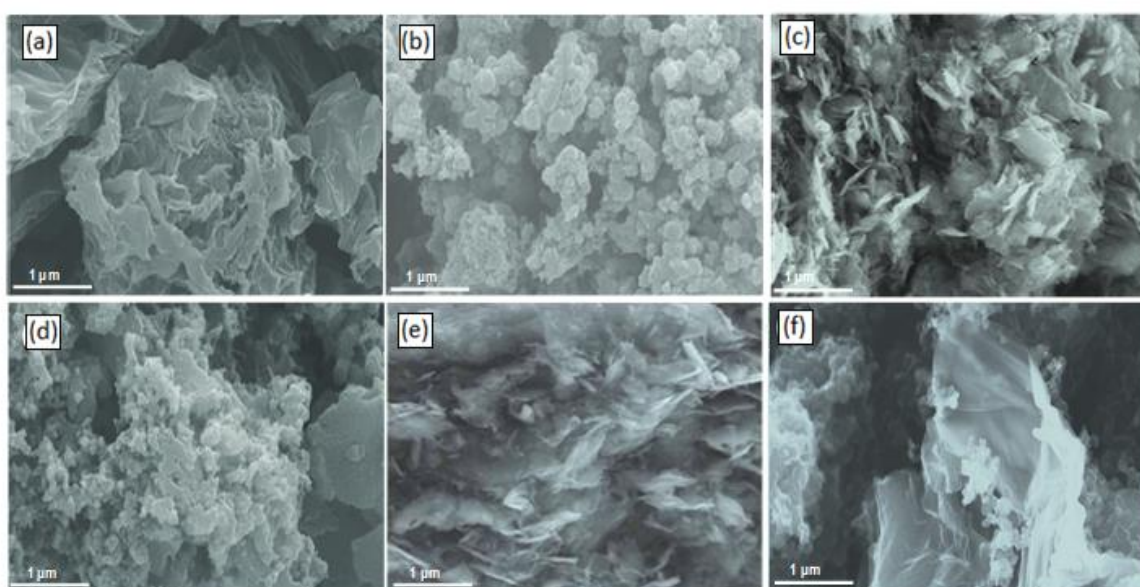


Figure 1. SEM micrographs of samples: raw GO (a), neat PANI (b), HDI-GO 6 (c), PANI/HDI-GO 6 (10 wt%) (d), HDI-GO 1 (e), and PANI/HDI-GO 1 (10 wt%) (f). Taken from [6].

The images of HDI-GO 6 reveals a stacked structure of graphene flakes, attributed to the linking between HDI chains and the GO surface due to the functional groups. The samples appear heterogeneous, since they comprise a mixture of raw GO sheets and HDI modified sheets; similar morphology was found for the HDI-GO 1 samples.

However, when the GO based materials are mixed with PANI particles, surfaces fully covered by PANI were observed. This result is consistent with previous works [21], since the use of HCl produces the adsorption of PANI in the graphene surface by electrostatic attraction. Furthermore, given that the HDI-GO has negative charge, it is expected that the PANI would be stick to the surface stronger due to the positive charge of PANI emeraldine salt form. Also, other kinds of interactions between PANI and HDI-GO structures can take place, such as pi-pi stacking, hydrophobic interactions and hydrogen bonding.

The polymerization method produced that the polymeric matrix covered the HDI-GO surface homogenously. This fact allows to yield composites in which the intercalation of HDI-GO in PANI is effective and no-agglomeration or phase separation takes place, in contrast with previous works [22,23]. The spaced layers of HDI-GO enable the diffusion on PANI particles between them, and later its deposition onto the surface as a thin coating.

Similar morphology was observed for all the nanocomposites with HDI-GO. The samples with HDI-GO 6 present a smooth surface, and a direct relation between the nanomaterial amount and degree of interpenetration. The arbitrarily distribution of graphene flakes onto the PANI matrix can be a potential aid to create conductive paths though the material. However, the sample with 10 wt% HDI-GO 1 presents a lower interpenetration structure. The GO sheets were more spaced due to the addition of PANI particles, which implies a larger level of exfoliation.

3.2. XRD Patterns

The XRD patterns prove the viability of the in situ polymerization method presented. The sample of pure PANI shows a peak at $2\theta = 25.3^\circ$, which is also presented in the diffractograms of every nanocomposite, but at lower 2θ and with lower intensity. This fact is explained considering the loading of nanomaterial [25]: the higher the amount of GO, the lower intensity and the lower 2θ .

Furthermore, the downshift was more noticeable for the samples with HDI-GO compared with those with GO, and also more marked with higher FD. As this shift is related with the interlayer distance, it is reasonable to think that the sample with higher amount of HDI will have the flakes more separated can hold more PANI particles in their surface and between layers.

In the case of GO, the interlayer is smaller than in the HDI-GO samples (for 10 wt%: 0.8 nm, vs. 1.18 nm (HDI-GO1) or 1.33 nm (HDI-GO6)). This is another fact that supports the idea of higher interlayer spacing implying higher intercalation of polymeric chains.

3.3. Raman Spectroscopy Results

The characteristic peaks of PANI (400–1800 cm^{-1}) and GO (disorder D band at 1345 cm^{-1} , and tangential G band at 1595 cm^{-1}) can be observed in the nanocomposites spectra. Also, the HDI-GO spectrum shows similar peaks than GO, but more intense due to the increased number of defects related to HDI and upshifted, attributed to a change in the electronic structure of GO in the presence of electron-acceptor groups [34]. Furthermore, the ratio between the intensity of the D and G band is indicative of the disorder [35]: the higher the ratio, the higher the number of defects; this ratio is about one for GO, meanwhile for the HDI-GO1 is 1.55 and HDI-GO6 is 1.73.

The spectra of the nanocomposites are similar to that of PANI, but the peaks are slightly shifted to higher wavelengths and their intensity is reduced. There are differences when comparing PANI/GO and PANI/HDI-GO samples: those with GO present a small upshift of the bands while PANI/HDI-GO1 and PANI/HDI-GO6 samples exhibit a strong upshift. These results are yet another confirmation for the presence of PANI chains on the GO or HDI-GO surface. Furthermore, the FD has an effect in the peaks: the higher the FD, the larger the modification of the peaks.

3.4. Thermal Stability

The thermal decomposition of the samples was investigated by TGA experiments under nitrogen atmosphere, and the thermographs are presented in Figure 2.

Some similarity can be observed by comparing PANI, GO and HDI-GO samples with the PANI/GO and PANI/HDI-GO composites.

PANI presents a first decomposition step related to a deprotonation, probably caused by the HCl molecules of the dopant [33], and a second step due to the elimination of the groups attached to the PANI backbone. The GO sample only shows one step around 250 °C, and it is attributed to the removal of functional groups [18]. HDI-GO also presents two steps: the first is related to the decomposition of the remaining functional groups, and the second correlates with the decomposition of HDI chains.

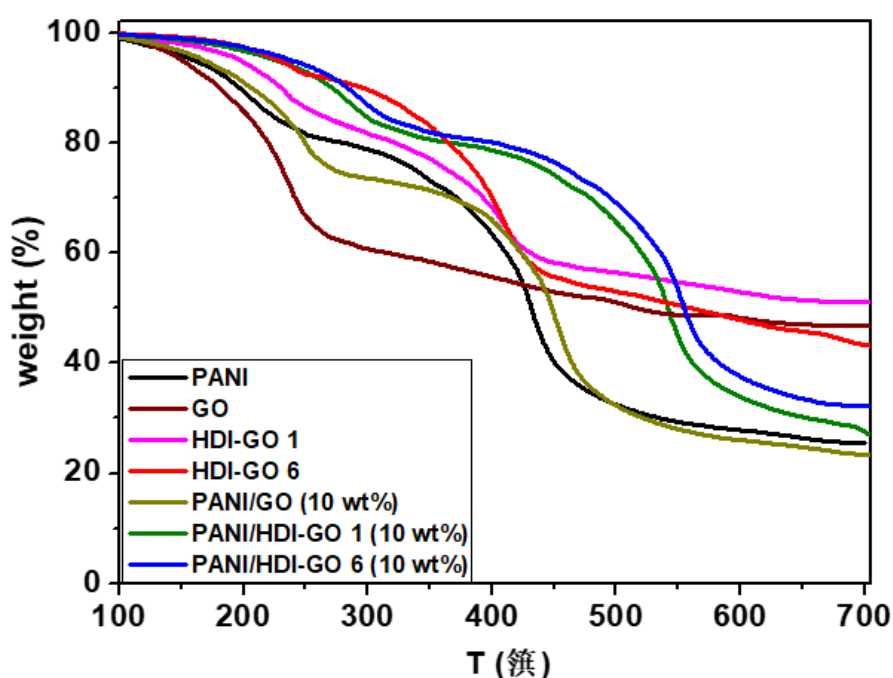


Figure 2. TGA curves under inert atmosphere of neat PANI, GO, HDI-GO 1, HDI-GO 6, and the nanocomposites with 10 wt% nanofiller loading. Taken from [6].

The thermographs of nanocomposites present two steps of degradation, like PANI, but with a higher thermal stability. These significant changes, larger in HDI-GO samples, implies that the addition of GO and HDI-GO nanomaterials to a PANI matrix improves the stability of the samples, increasing the degradation temperatures in every step. This improvement can be related with the PANI/HDI-GO interaction. The HDI-GO flakes protect PANI from the heat. This kind of stability enhancement was previously reported for PANI/graphene nanoplatelets [36]. Furthermore, it can be observed that the higher the loading of HDI-GO, the higher the thermal stability, and also the higher FD, the higher stability. This fact can be explained considering that the strong interactions between PANI and HDI-GO restrains the polymeric rotational movement, so the stability is improved.

4. Conclusions

In this work nanocomposites based on PANI/HDI-GO mixtures were prepared; the synthesis involved an in-situ polymerization of aniline monomers with HDI-GO nanofillers in acid medium with $(\text{NH}_4)_2\text{S}_2\text{O}_8$ as oxidizing agent. In order to study the effect of HDI-GO on the properties of the nanocomposites, the samples were characterized by different techniques. Experimental results show that the samples morphology consists in a dense network of PANI matrix particles deposited onto

the GO-based materials surface. The interactions between PANI and HDI-GO are mainly hydrogen bonding, pi-pi stacking, electrostatic and hydrophobic interactions. It was noticed that the higher the concentration of HDI-GO, the higher the thermal stability and the electrical conductivity of PANI composites; further, the conductivity also increased with increasing HDI-GO functionalization degree. This new procedure for synthesizing PANI/HDI-GO nanocomposites offers the opportunity of developing new multifunctional graphene/polymer-based materials for a broad range of applications.

Author Contributions: J.A.L.-S. performed the experiments; A.M.D.P. wrote the paper. All authors have read and agreed to the published version of the manuscript.

Acknowledgments: J.A. Luceño-Sanchez wishes to acknowledge the University of Alcalá for a “Formación de Personal Investigador (FPI)” PhD fellowship.

Conflicts of Interest: The authors declare no conflict of interest.

References

1. Li, D.; Huang, J.; Kaner, R.B. Polyaniline Nanofibers: A Unique Polymer Nanostructure for Versatile Applications. *Acc. Chem. Res.* **2009**, *42*, 135–145, doi:10.1021/ar800080n.
2. Bhadra, S.; Khashtgir, D.; Singha, N.K.; Lee, J.H. Progress in preparation, processing and applications of polyaniline. *Prog. Polym. Sci.* **2009**, *34*, 783–810, doi:10.1016/j.progpolymsci.2009.04.003.
3. Díez-Pascual, A.M.; Luceño Sanchez, J.A.; Peña Capilla, R.; García Díaz, P. Recent Developments in Graphene/Polymer Nanocomposites for Application in Polymer Solar Cells. *Polymers* **2018**, *10*, 217, doi:10.3390/polym10020217.
4. Wang, L.; Lu, X.; Lei, S.; Song, Y. Graphene-based polyaniline nanocomposites: Preparation, properties and applications. *J. Mater. Chem. A* **2014**, *2*, 4491–4509, doi:10.1039/C3TA13462H.
5. Boeva, Z.; Sergeev, V. Polyaniline: Synthesis, properties, and application. *Polym. Sci. Ser. C* **2014**, *56*, 144–153, doi:10.1134/S1811238214010032.
6. Luceño Sánchez, J.A.; Díez-Pascual, A.M.; Peña Capilla, R.; García Díaz, P. The Effect of Hexamethylene Diisocyanate-Modified Graphene Oxide as a Nanofiller Material on the Properties of Conductive Polyaniline. *Polymers* **2019**, *11*, 1032.
7. Huang, J.; Kaner, R.B. Nanofiber Formation in the Chemical Polymerization of Aniline: A Mechanistic Study. *Angew. Chem. Int. Ed.* **2004**, *43*, 5817–5821, doi:10.1002/anie.200460616.
8. Peng, C.; Zhang, S.; Jewell, D.; Chen, G.Z. Carbon nanotube and conducting polymer composites for supercapacitors. *Prog. Nat. Sci.* **2008**, *18*, 777–788, doi:10.1016/j.pnsc.2008.03.002.
9. Yan, J.; Wei, T.; Shao, B.; Fan, Z.; Qian, W.; Zhang, M.; Wei, F. Preparation of a graphene nanosheet/polyaniline composite with high specific capacitance. *Carbon* **2010**, *48*, 487–493, doi:10.1016/j.carbon.2009.09.066.
10. Liu, Y.; Zhou, J.; Zhang, X.; Liu, Z.; Wan, X.; Tian, J.; Wang, T.; Chen, Y. Synthesis, characterization and optical limiting property of covalently oligothiophene-functionalized graphene material. *Carbon* **2009**, *47*, 3113–3121, doi:10.1016/j.carbon.2009.07.027.
11. Bai, H.; Xu, Y.; Zhao, L.; Li, C.; Shi, G. Non-covalent functionalization of graphene sheets by sulfonated polyaniline. *Chem. Commun.* **2009**, 1667–1669, doi:10.1039/B821805F.
12. Wu, Q.; Xu, Y.; Yao, Z.; Liu, A.; Shi, G. Supercapacitors Based on Flexible Graphene/Polyaniline Nanofiber Composite Films. *ACS Nano* **2010**, *4*, 1963–1970, doi:10.1021/nn1000035.
13. Gedela, V.R.; Srikanth, V.V.S.S. Electrochemically active polyaniline nanofibers (PANi NFs) coated graphene nanosheets/PANi NFs composite coated on different flexible substrates. *Synth. Met.* **2014**, *193*, 71–76, doi:10.1016/j.synthmet.2014.03.030.
14. Xu, J.; Wang, K.; Zu, S.; Han, B.; Wei, Z. Hierarchical Nanocomposites of Polyaniline Nanowire Arrays on Graphene Oxide Sheets with Synergistic Effect for Energy Storage. *ACS Nano* **2010**, *4*, 5019–5026, doi:10.1021/nn1006539.
15. Wu, W.; Li, Y.; Yang, L.; Ma, Y.; Pan, D.; Li, Y. A Facile One-Pot Preparation of Dialdehyde Starch Reduced Graphene Oxide/Polyaniline Composite for Supercapacitors. *Electrochim. Acta* **2014**, *139*, 117–126, doi:10.1016/j.electacta.2014.06.166.
16. Kumar, N.A.; Choi, H.; Shin, Y.R.; Chang, D.W.; Dai, L.; Baek, J. Polyaniline-Grafted Reduced Graphene Oxide for Efficient Electrochemical Supercapacitors. *ACS Nano* **2012**, *6*, 1715–1723, doi:10.1021/nn204688c.

17. Díez-Pascual, A.M.; Díez-Vicente, A.L. Poly(propylene fumarate)/Polyethylene Glycol-Modified Graphene Oxide Nanocomposites for Tissue Engineering. *ACS Appl. Mater. Interfaces* **2016**, *8*, 17902–17914, doi:10.1021/acsami.6b05635.
18. Luceño-Sánchez, J.A.; Maties, G.; Gonzalez-Arellano, C.; Díez-Pascual, A.M. Synthesis and Characterization of Graphene Oxide Derivatives via Functionalization Reaction with Hexamethylene Diisocyanate. *Nanomaterials* **2018**, *8*, 870, doi:10.3390/nano8110870.
19. Luceño Sánchez, J.A.; Peña Capilla, R.; Díez-Pascual, A.M. High-Performance PEDOT:PSS/Hexamethylene Diisocyanate-Functionalized Graphene Oxide Nanocomposites: Preparation and Properties. *Polymers* **2018**, *10*, 1169, doi:10.3390/polym10101169.
20. Stejskal, J.; Sapurina, I.; Trchová, M. Polyaniline nanostructures and the role of aniline oligomers in their formation. *Prog. Polym. Sci.* **2010**, *35*, 1420–1481, doi:10.1016/j.progpolymsci.2010.07.006.
21. Du, X.S.; Xiao, M.; Meng, Y.Z. Facile synthesis of highly conductive polyaniline/graphite nanocomposites. *Eur. Polym. J.* **2004**, *40*, 1489–1493, doi:10.1016/j.eurpolymj.2004.02.009.
22. Male, U.; Srinivasan, P.; Singu, B.S. Incorporation of polyaniline nanofibres on graphene oxide by interfacial polymerization pathway for supercapacitor. *Int. Nano Lett.* **2015**, *5*, 231–240, doi:10.1007/s40089-015-0160-9.
23. Thomas, S.; Zaikov, G.E.; Valsaraj, S.V. *Recent Advances in Polymer Nanocomposites*, 1st ed.; CRC Press: Baton Rouge, LA, USA, 2009; p. 110. ISBN 9789004167261.
24. Vallés, C.; Jiménez, P.; Muñoz, E.; Benito, A.M.; Maser, W.K. Simultaneous Reduction of Graphene Oxide and Polyaniline: Doping-Assisted Formation of a Solid-State Charge-Transfer Complex. *J. Phys. Chem. C* **2011**, *115*, 10468–10474, doi:10.1021/jp201791h.
25. Muralikrishna, S.; Nagaraju, D.H.; Balakrishna, R.G.; Surareungchai, W.; Ramakrishnappa, T.; Shivanandareddy, A.B. Hydrogels of polyaniline with graphene oxide for highly sensitive electrochemical determination of lead ions. *Anal. Chim. Acta* **2017**, *990*, 67–77, doi:10.1016/j.aca.2017.09.008.
26. Solonaru, A.M.; Grigoras, M. Water-soluble polyaniline/graphene composites as materials for energy storage applications. *Express Polym. Lett.* **2017**, *11*, 127–139, doi:10.3144/expresspolymlett.2017.14.
27. Kou, L.; He, H.; Gao, C. Click chemistry approach to functionalize two-dimensional macromolecules of graphene oxide nanosheets. *Nano-Micro Lett.* **2010**, *2*, 177–183, doi:10.1007/BF03353638.
28. Alexander, L.E. *X-ray diffraction methods in polymer science*; Wiley-Interscience: New York, NY, USA, 1969; ISBN 9780471021834.
29. Díez-Pascual, A.M.; Ferreira, C.H.; Andrés, M.P.S.; Valiente, M.; Vera, S. Effect of Graphene and Graphene Oxide Dispersions in Poloxamer-407 on the Fluorescence of Riboflavin: A Comparative Study. *J. Phys. Chem. C* **2017**, *121*, 830–843, doi:10.1021/acs.jpcc.6b09800.
30. Wang, C.; Feng, L.; Yang, H.; Xin, G.; Li, W.; Zheng, J.; Tian, W.; Li, X. Graphene oxide stabilized polyethylene glycol for heat storage. *Phys. Chem. Chem. Phys.* **2012**, *14*, 13233–13238, doi:10.1039/C2CP41988B.
31. Vargas, L.R.; de Souza, C.B.; Poli, A.K.S.; Duta, R.C.L.; Baldan, M.R.; Gonçalves, E.S. Formation of Composite Polyaniline and Graphene Oxide by Physical Mixture Method. *J. Aerosp. Technol. Manag.* **2017**, *9*, 29–38, doi:10.5028/jatm.v9i1.697.
32. Grzeszczuk, M.; Grańska, A.; Szostak, R. Raman spectroelectrochemistry of polyaniline synthesized using different electrolytic regimes-multivariate analysis. *Int. J. Electrochem. Sci.* **2013**, *8*, 8951–8965.
33. Šeděnková, I.; Trchová, M.; Stejskal, J. Thermal degradation of polyaniline films prepared in solutions of strong and weak acids and in water – FTIR and Raman spectroscopic studies. *Polym. Degrad. Stabil.* **2008**, *93*, 2147–2157, doi:10.1016/j.polymdegradstab.2008.08.007.
34. Díez-Pascual, A.M.; Vallés, C.; Mateos, R.; Vera-López, S.; Kinloch, I.A.; Andrés, M.P.S. Influence of surfactants of different nature and chain length on the morphology, thermal stability and sheet resistance of graphene. *Soft Matter* **2018**, *14*, 6013–6023, doi:10.1039/C8SM01017J.
35. Dresselhaus, M.S.; Jorio, A.; Filho, A.G.S.; Saito, R. Defect characterization in graphene and carbon nanotubes using Raman spectroscopy. *Philos. Trans. A Math. Phys. Eng. Sci.* **2010**, *368*, 5355–5377, doi:10.1098/rsta.2010.0213.
36. Gedela, V.R.; Srikanth, V.V.S.S. Electrochemically active polyaniline nanofibers (PANi NFs) coated graphene nanosheets/PANi NFs composite coated on different flexible substrates. *Synth. Met.* **2014**, *193*, 71–76, doi:10.1016/j.synthmet.2014.03.030.

Publisher's Note: MDPI stays neutral with regard to jurisdictional claims in published maps and institutional affiliations.



© 2020 by the authors. Submitted for possible open access publication under the terms and conditions of the Creative Commons Attribution (CC BY) license (<http://creativecommons.org/licenses/by/4.0/>).